A Genetic Network That Balances Two Outcomes Utilizes Asymmetric Recognition of Operator Sites

Abhishek Mazumder,[†] Sumita Bandyopadhyay,[‡] Amlanjyoti Dhar,[¶] Dale E. A. Lewis,[¶] Sunanda Deb,[‡] Sucharita Dey,[§] Pinak Chakrabarti,[§] and Siddhartha Roy[†*]

[†]Division of Structural Biology and Bioinformatics, Council of Scientific and Industrial Research-Indian Institute of Chemical Biology, Calcutta, India; [‡]Department of Biophysics and [§]Department of Biochemistry, Bose Institute, Calcutta, India; and [¶]Laboratory of Molecular Biology, National Cancer Institute, Bethesda, Maryland

ABSTRACT Stability and induction of the lysogenic state of bacteriophage λ are balanced by a complex regulatory network. A key feature of this network is the mutually exclusive cooperative binding of a repressor dimer (CI) to one of two pairs of binding sites, O_R1-O_R2 or O_R2-O_R3. The structural features that underpin the mutually exclusive binding mode are not well understood. Recent studies have demonstrated that CI is an asymmetric dimer. The functional importance of the asymmetry is not fully clear. Due to the asymmetric nature of the CI dimer as well as its binding sites, there are two possible bound orientations. By fluorescence resonance energy transfer measurements we showed that CI prefers one bound orientation. We also demonstrated that the relative configuration of the binding sites is important for CI dimer-dimer interactions and consequent cooperative binding. We proposed that the operator configuration dictates the orientations of the bound CI molecules, which in turn dictates CI cooperative interaction between the O_R1-O_R2 or O_R2-O_R3, but not both. Modeling suggests that the relative orientation of the C- and N-terminal domains may play an important role in the mutually exclusive nature of the cooperative binding. This work correlates unique structural features of a transcription regulatory protein with the functional properties of a gene regulatory network.

INTRODUCTION

Living organisms depend on myriads of correct and exquisitely sophisticated molecular interactions. Gene regulatory circuits, an important component of the living organisms, are multistate switches that are composed of protein-DNA and protein-protein interactions. How the multiple states of these switches are created from the basic levels of protein-protein and protein-DNA interactions are not well understood. With the advent of synthetic biology, attempts are being made to reach a more quantitative understanding of gene regulatory circuits to facilitate their design (1,2).

The temperate phages, like bacteriophage λ, can switch between two developmental states, lysis and lysogeny. The regulatory network of bacteriophage λ that switches between lytic and lysogenic developmental pathways has emerged as a model for complex regulatory networks (3,4). One major task of the regulatory genetic network of bacteriophage λ is to maintain a stable lysogenic state and provide ease of induction to a lytic pathway when required. A stable lysogenic state is maintained by multimeric complexes of CI cooperatively bound to a pair of operators, O_L and O_R, on the bacteriophage λ genome involving a long range looping (Fig. 1). It is generally believed that during lysogeny, an octameric complex is initially formed in which four dimers of CI are bound to O_R1-O_R2 and O_L1-O_L2 with concomitant looping of the intervening DNA (5). An important feature of the lysogenic state is the stimulation of the promoter, P_{RM}, to maintain the prophage state. Stimulated P_{RM} synthesizes more CI resulting in cooperative interaction of CI bound to O_R3 and O_L3, and the formation of an octameric plus tetrameric loop in which the P_{RM} is repressed (Fig. 1). The octameric and octameric plus tetrameric complexes are an important part of the lysogen stability and at the same time they play an important role in balancing the stability with induction (6,7). This complex switching behavior is regulated by feedback loops (Fig. 2 *A*). The positive autoregulation of the *cI* gene by the CI protein at low concentrations and negative autoregulation at high concentrations are important for keeping the CI concentration in a lysogenic cell within a narrow range, thus balancing the stable maintenance of lysogeny and induction. The stability of the intermediate octameric state is crucial for the positive autoregulation and is proposed to be underpinned by the inability of CI bound to O_R3 to make cooperative contacts with CI bound to O_R2 in the presence of CI bound to O_R1 as this would disrupt the octameric state. This mutually exclusive nature of cooperative binding has been termed alternate pairwise cooperativity, whose structural basis is not understood (6).

For many years, it was believed that, like other prokaryotic repressors, CI was a symmetric dimer participating in protein-protein interactions in the DNA-bound state, thus forming DNA loops like many other gene regulatory proteins. However, recent solution and crystal structure studies established that CI is an asymmetric dimer (8,9). This raises an important question as to the role of this structural asymmetry in the interaction network of CI and the underlying thermodynamic basis. In this article, we report that the configuration (For the purpose of this article, we

Submitted July 31, 2011, and accepted for publication January 27, 2012.

*Correspondence: sidroykolkata@gmail.com

Editor: Laura Finzi.

0006-3495/12/04/1580/10 $2.00

doi: 10.1016/j.bpj.2012.01.052

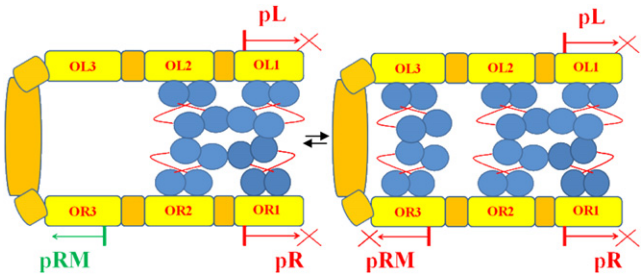

FIGURE 1 CI octamer (8-mer) versus octamer and tetramer loop (8 + 4-mer). The operator regions contain a subset of operator sites: (O_L-O_L1, O_L2, and O_L3) and (O_R-O_R1, O_R2, and O_R3). The regulatory region contains two lytic promoters (P_L and P_R) and a lysogenic promoter, P_{RM}. At low CI concentrations, the octamer liganded state is formed when CI tetramers at O_L1-O_L2 bind cooperatively to another tetramer bound at O_R1-O_R2 repressing P_L and P_R, and activating P_{RM}. At high CI concentrations, CI dimer bound to O_L3 binds cooperatively to another CI dimer at O_R3, repressing P_{RM}. The structure of the loop is not drawn to scale and the arrangement of the CI dimers in the loop is not known.

call the inversion of the binding sites (operator sites) as change of configuration, whereas the inversion of bound protein as change of orientation.) of O_R2 is critical for cooperative CI binding to O_R1-O_R2 and P_{RM} activation. We also report modeling of CI orientation on the operator, which suggests that the inversion of configuration of O_R2 (and consequent reorientation of the CI bound to O_R2) may put the two protein-protein interaction domains (C-terminal domain) of CI bound to O_R1 and O_R2 on the opposite faces of the DNA, making cooperative interaction unfavorable. Modeling also suggests that CI bound to O_R2 in the preferred orientation in the wild-type (WT) O_R2 configuration is not favored to interact with CI bound to O_R3, making cooperative binding of CI to O_R2-O_R3 unlikely. However, reorientation of CI bound to O_R2 would favor O_R2-O_R3 cooperativity, whereas abrogating O_R1-O_R2 cooperativity.

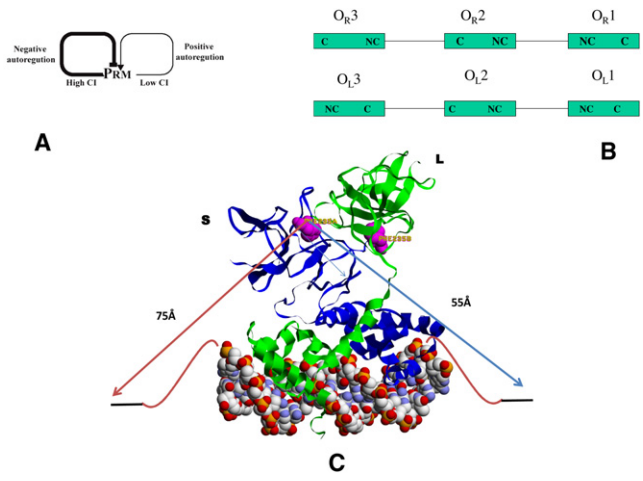

FIGURE 2 (*A*) Positive and negative autoregulation by CI. (*B*) The orientations of the operator sites in bacteriophage λ. Assignments of C and NC half-sites are based on Ptashne (6). (*C*) Model indicating the distances of Phe-235 of the subunit L from the ends of the DNA.

This was supported by fluorescence resonance energy transfer (FRET) data. Thus, we relate the functional properties of this network to unique structural features of the protein and its DNA binding sites.

MATERIALS AND METHODS

Details of the methods are given in the Supporting Material.

Purification

λ-Repressor (CI) was purified according to Banik et al. (10). Phe-235-Cys repressor was purified according to Bandyopadhyay et al. (9). Some of the oligonucleotides were purchased from TriLink (San Diego, CA), whereas others were synthesized on an Applied Biosystems (Carlsbad, C A) 3400 DNA Synthesizer. Sequences of the oligonucleotides with or without aminolink are given in Table S1. The oligonucleotides were purified as described previously (11).

Chemical modifications

Oligonucleotides with 5′-C6 aminolink were labeled with fluorescein isothiocyanate or eosin isothiocyanate (dissolved in *N,N*-dimethylformamide) in 200 μl solution containing 1 M sodium carbonate/bicarbonate buffer, pH 9.0: *N,N*-dimethylformamide: water in the ratio 5:2:3 as described previously (12).

FRET

For FRET experiments, energy transfer efficiency, E, was calculated from excitation spectra using the following equation (13):

$$\frac{F_{D+A}}{F_A} = 1 + \left(\frac{\varepsilon_D C_D}{\varepsilon_A C_A}\right) E.$$

Distance estimates were obtained as described previously (14).

Circular dichroism

Circular dichroism (CD) measurements were done on a JASCO (Tokyo, Japan) J850 spectropolarimeter using a 1 cm pathlength quartz cuvette, according to Bandyopadhyay et al. (15).

Isothermal titration calorimetry

All experiments were done in a VP-ITC instrument from Microcal (Northampton, MA) according to Merabet and Ackers (16).

In vitro transcription reactions

In vitro transcription assays were performed as described by Lewis et al. (17). Sequences of P_{RM}-O_R-P_R templates used in this study are given in Table S2.

RESULTS

CI preferentially binds operator sites in one orientation

The operator site sequences in the phage λ genome are not perfectly symmetric and consist of the consensus (called C here) and nonconsensus (called NC here) half-sites (6).

The designation of the C half-site refers to the half-site within an operator site that deviate the least from the consensus half-site sequence as given by Ptashne (6). Both O_R1-O_R2 and O_L1-O_L2 site pairs are configured in such a manner that the NC half-sites face each other (NC-NC arrangement), whereas in O_R2-O_R3 and O_L2-O_L3, the half-sites arrangements are C-NC and C-C, respectively (Fig. 2 *B*). A previous solution study and a recent crystal structure of CI-DNA complex (8) showed that the two chemically identical subunits of CI dimer are in different conformations. The conformational nonequivalence of the two subunits implies two possible orientations on the nonsymmetric operator site of which only one orientation is seen in the crystal. However, the process of crystallization may trap one of the orientations present; thus, we cannot rule out the absence of other orientations of the protein bound to the operator site. One way to investigate the orientation of the asymmetric protein on the asymmetric operator site is through measurement of the distance between a selected locus of the protein and a selected locus of the DNA by FRET experiments. In the crystal structure, the two CI subunits cross each other near the hinge regions putting the C-terminal domain of the subunit that binds to the consensus half-site spatially near the nonconsensus half-site of the operator site and vice versa (8). However, the last few residues of the C-terminal tail region (residues 228–236) go across again toward the other half-site, thus bringing that region of the C-terminus tail closer to the half-site that bound the N-terminal domain (Fig. 2 *C*). Conformation of each subunit is different from the other in the crystal structure. One of them has a more compact hinge (residues 93–122) with an interresidue distance of 26 Å (S for short-hinge). The hinge length in the green subunit is 39 Å (L for long-hinge). In the crystal structure, the S subunit interacts with the C half-site. Previously, we created a unique fluorescence probe attachment point in the protein by site-directed mutagenesis (Phe-235-Cys). This cysteine showed half-of-the-site reactivity most likely because Cys-235 residue from only one subunit reacts (in the free state). However, it is not known whether the reactive Cys-235, and hence the labeled fluorescent probe, is on S or the L subunit.

Fig. 2 *C* shows the crystal structure of the protein and the approximate locations of Phe-235 (atom Cγ) and the terminal 5′-phosphate near the C and the NC half-sites. The distance between Phe-235 (subunit S) and 5′-terminal phosphate at the C-end is 43 Å, and between the same Phe-235 and NC-end phosphate is 56 Å; the distance between Phe-235 in the subunit L and C-end phosphate is 55 Å and between the same Phe-235 and NC-end phosphate is 42 Å. If the orientation of the CI, labeled at a single subunit, on the operator site is unique (i.e., only one of the two possible orientations are present), then the distance measured by FRET between the fluorescent probe at Cys-235 (labeled at a single subunit only) and a probe placed on the 5′end of one of the DNA strands will be different between Cys-235:5′-C-end and Cys-235:5′-NC-end. If both orientations were equally probable, the measured distance would be the average of the distances in the two orientations and would yield the same value. We attempted to measure the FRET between acrylodan (FRET donor) labeled Phe-235-Cys CI (labeled at one subunit) and a 29-mer duplex oligonucleotide containing O_R1 sequence in which the eosine (FRET acceptor) is placed near the 5′-NC-end or the 5′-C-end through a synthetic hexylamine linker. Because we used a longer O_R1 duplex than the one used in the crystal structure, we attempted to estimate the distances in the duplex, using simple modeling and calculation. This showed that the addition of five basepairs and the hexylamine linker at each end makes the distances of the probe from subunit S to the C-end ~55 Å and to the NC-end ~75 Å. Similarly, the distance from Phe-235 on the L subunit to NC end is ~55 Å and to the C-end is 75 Å (Fig. 2 *C*). Comparison of excitation spectra of the one-end eosine labeled DNA duplex, complexed with acrylodan-labeled and unlabeled Phe-235-Cys CI were clearly different when the labels are at the different ends of the oligonucleotide duplex (Fig. 3, *A* and *B*). For the NC-end labeled duplex the fluorescence intensity around the peaks of the donor absorption wavelengths (around 360 nm) is higher in the acrylodan-labeled protein complex than the unlabeled protein complex. The calculated FRET distance was 59 Å. In the corresponding spectral comparison, when the label was near the C-end, the difference between the two spectra was negligible and the calculated distance is $>$75 Å (as the energy transfer efficiency is insignificant). These derived distances are consistent with the reactive cysteine being on the L subunit and the orientation being the same as that seen in the crystal.

WT configuration of O_R2 is required for cooperativity

If the previous relative orientation of the CI-operator complex is energetically favored, as suggested by FRET experiments, in both O_R1 and O_R2 cases, the C-terminal domains of the two S subunits on natural O_R1-O_R2 double operator sites/CI tetramer complex will then face each other (due to chain crossover) and this arrangement may be required for cooperative interaction (C-NC-NC-C arrangement) (Figs. 1 and 2 *B*). If the sequence of O_R2 is inverted (referred to here as O_R2^{inv}) around its pseudosymmetry axis in the DNA containing both O_R1 and O_R2, it will then create a C-NC-C-NC configuration (O_R1-O_R2^{inv} arrangement without changing the actual O_R2 sequence). This arrangement may be unfavorable for CI cooperativity if the configuration of the operator sites is important for protein-protein interactions. Previously, we have demonstrated that cooperative binding of CI to a DNA duplex containing WT O_R1-O_R2, leads to change in CD of the DNA,

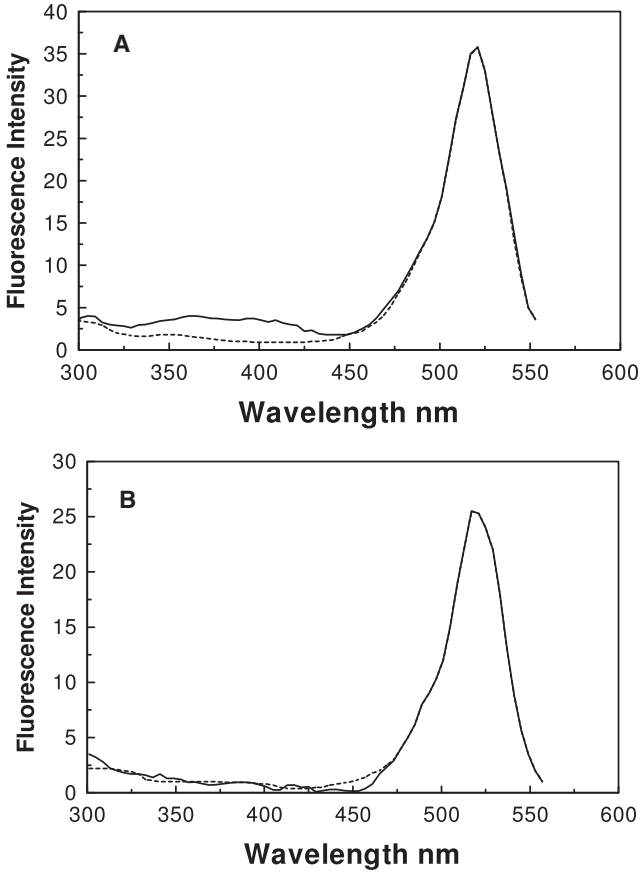

FIGURE 3 FRET between acrylodan-labeled Phe-235-Cys repressor and one-end eosine labeled 29 basepair oligonucleotide duplex containing O_R1 sequence mixed in the ratio of 2(monomer):1(duplex). (*A*) The excitation spectra of eosine-O_R1 (NC-end)/acrylodan-Phe-235-Cys repressor complex (*solid line*) and eosin-O_R1 (NC-end)/Phe-235-Cys repressor complex (*dotted line*). (*B*) The excitation spectra of eosine-O_R1 (C-end)/acrylodan-Phe-235-Cys repressor complex (*solid line*) and eosin-O_R1 (C-end)/Phe-235-Cys repressor complex (*dotted line*).

suggesting a distortion of the DNA structure (15). This distortion was in the interoperator spacer DNA and was also seen in footprinting experiments (18). Annulment of cooperative interaction by insertion of half-turn of DNA between O_R1 and O_R2 also led to abrogation of the change of DNA CD, as well. Thus, the change of DNA CD spectra is a sensitive indicator of the cooperative interaction of CI to O_R1-O_R2. Fig. 4, *A* and *B*, show the CD spectra for O_R1-O_R2 and O_R1-O_R2^{inv} in the presence and absence of a stoichiometric amount of repressor. WT O_R1-O_R2 showed significant change in DNA CD spectra, whereas O_R1-O_R2^{inv} showed a much reduced magnitude of change. We studied DNA CD of a control O_R1-O_R2 in which four additional basepairs are inserted between the two operator sites (referred to here as O_R1-(+4)-O_R2) (Fig. 4 *C*). The two CD spectra were similar indicating CI cooperativity was interrupted in both cases. In O_R1^{inv}-O_R2, where O_R1 was inverted, the CD difference is similar to that of the O_R1-O_R2, indicating the presence of cooperative interaction (Fig. 4 *D*). The magnitude of the differences at 265 nm was 0.85 mdeg for WT, 0.9 mdeg for O_R1^{inv}-O_R2, 0.4 mdeg for O_R1-O_R2^{inv}, and 0.28 mdeg for the O_R1-(+4)-O_R2. A smaller change of DNA CD in O_R1^{inv}-O_R2 and O_R1-(+4)-O_R2, compared to WT O_R1-O_R2 and O_R1-O_R2^{inv}, was probably due to distortion in O_R2 upon CI binding (as was observed in single O_R2 binding; data not shown). These differences are consistently reproduced. The reduced change in CD spectra suggests a reduced DNA distortion in the O_R1-O_R2^{inv} upon CI binding. This reduction in DNA distortion in the latter may originate from a lack of protein-protein contact or from a more favorable geometry of the protein interfaces in which the DNA distortion is no longer required to establish protein-protein contact. These alternatives can be distinguished by binding isotherms.

CI cooperative binding increases the individual site occupancy as was demonstrated by Ptashne (6), Ackers and colleagues (19–21). WT O_R1-O_R2 is expected to have the highest cooperativity, and any change in the orientation of O_R1 or O_R2 that disrupt protein-protein interaction will result in reduced cooperativity. Hence, the loss of cooperative contact will reduce the apparent affinity of CI toward a DNA duplex containing both O_R1 and O_R2 in WT orientation. To investigate cooperativity between CI at O_R1 and O_R2 by electrophoretic mobility shift, we mutated O_R3 in the following templates: O_R1-O_R2, O_R1^{inv}-O_R2 and O_R1-O_R2^{inv} (Fig. S3). The mutated O_R3 eliminates the possibility of cooperative interaction of CI between O_R2-O_R3. The CI-DNA complex in the three cases was observed around 40 nM of CI and >50% of free DNA was bound at ~80 nM CI as was evident from band shifts (Fig. S3). CI binding cooperativity was determined from Hill plots. Under the solution conditions, CI binding to the DNA and consequent band shift occurs around 40 nM CI concentrations, overlapping with the dimer-monomer dissociation constant of the CI (22). Thus, binding is coupled to monomer-dimer association and should show a Hill coefficient of ~2 in the absence of any dimer-dimer interaction and consequent cooperativity. The Hill coefficient determined from the Hill plot was 1.9 for O_R1-O_R2^{inv}, indicating no dimer-dimer interaction. For O_R1-O_R2, the Hill coefficient was 3.02, indicating the presence of significant dimer-dimer interaction and cooperativity. For O_R1^{inv}-O_R2, the Hill coefficient was 2.24, indicating the presence of some residual cooperativity.

A more quantitative binding isotherm was determined using fluorescence anisotropy and isothermal titration calorimetry. We used an end-labeled DNA duplex containing either O_R1-O_R2, O_R1^{inv}-O_R2, O_R1-O_R2^{inv} or O_R1-(+4)-O_R2, for quantifying CI binding by fluorescence anisotropy. Although individual site binding cannot be resolved under such conditions, this reduction of overall binding affinity in O_R1-(+4)-O_R2 in comparison to that in O_R1-O_R2 is a good indication of the loss of cooperativity (for thermodynamic justification, see Annexure I of the Supporting

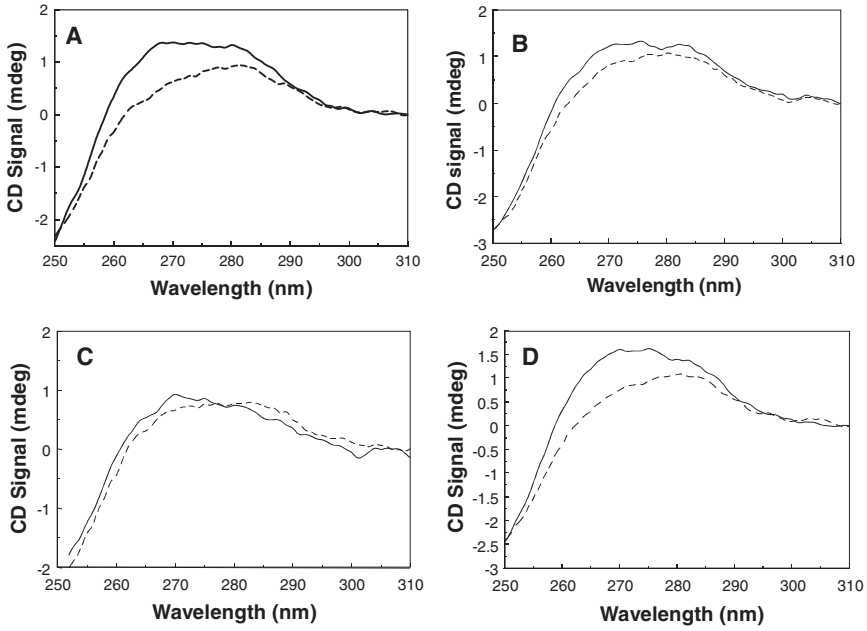

FIGURE 4 Difference CD spectra of (*A*) WT O_R1-O_R2; (*B*) O_R1-O_R2^{inv}; (*C*) four basepair inserted O_R1-O_R2 (O_R1-(+4)-O_R2); and (*D*) O_R1^{inv}-O_R2; all in the presence (*solid line*) and in the absence (*dashed*) of a stoichiometric amount of CI. The CD spectra of oligonucleotides and the oligonucleotide complexes were taken at oligonucleotide concentrations of 0.25 μM and protein concentrations of 1.0 μM, respectively.

Material). Fig. 5 *A* shows the CI binding isotherms of O_R1-O_R2, O_R1^{inv}-O_R2, O_R1-O_R2^{inv}, and O_R1-(+4)-O_R2 templates. The data were fitted to a two-site binding equation (a slightly modified version of Eq. 10 in the Supporting Material; because this equation ignores the dimer-monomer dissociation, the pH 8.0 binding data were used to extract α-values as the binding at pH 8.0 is weaker and hence the operator site binding occurs mostly at concentrations higher than the dimer-monomer dissociation constant). The extracted α-values (higher values indicate a higher degree of cooperativity and a value of 1 indicates no cooperativity) were 11.3, 1.08, 10.6, and 1.0 for O_R1-O_R2, O_R1-O_R2^{inv}, O_R1^{inv}-O_R2, and O_R1-(+4)-O_R2, respectively. The result was consistent with the loss of cooperative interaction between CI dimers bound to O_R1 and O_R2 upon the inversion of O_R2 (O_R1-O_R2^{inv}). This is consistent with the loss of cooperative interaction between O_R1 and O_R2 bound CI dimers upon inversion of O_R2. However, a significant degree of cooperativity was preserved in O_R1^{inv}-O_R2.

Isothermal titration microcalorimetry was previously used to measure CI binding to lambda operator sites by Merabet and Ackers (16). Fig. 5 *B* shows the ΔH versus ligand/protein ratio plot of O_R1-O_R2 and O_R1-O_R2^{inv} from similar isothermal titration microcalorimetry measurements. As a noncooperative control, O_R1-(+4)-O_R2 DNA was chosen. In these experiments, increasing concentrations of DNA were added to 2 μM CI present in the cell (16), with CI being in excess initially. By further addition of DNA, excess operator sites over CI were reached. For O_R1-O_R2, both sites on the same DNA molecule will be occupied simultaneously, due to cooperativity. When excess oligonucleotide is present, repressor will not be redistributed to excess O_R1 sites as the free energy difference between O_R1 and O_R2 binding is less than the loss of cooperative interaction energy (23,24). Thus, the binding isotherm should saturate at ~0.25 of DNA/CI monomer ratio as was observed in Fig. 5 *B*. For the O_R1-(+4)-O_R2 template with no binding cooperativity, the interpretation of binding curve was complex because at excess DNA, the CI initially bound to O_R2 in the CI excess regime probably redistributes to O_R1. The observed saturation point at excess DNA was around 0.5 as expected for CI bound to O_R1. The O_R1-O_R2^{inv} operator behaved very similar to O_R1-(+4)-O_R2 and hence shows no CI cooperative binding. If the isotherms were fitted to a single-site binding equation, the derived average binding affinity of O_R1-O_R2 is 10 nM. This is in reasonable agreement with the fluorescence anisotropy data.

O_R2 orientation is crucial for P_{RM} activation

The experiments described previously demonstrated that the orientation of the asymmetric CI dimer at O_R2 is crucial for cooperative interaction of CI at O_R1-O_R2. Therefore, we decided to investigate the effect of the O_R2 inversion on transcription from the λ lysogenic promoter, P_{RM}, which should be stimulated by CI bound to O_R2 (25). The DNA templates, which contain O_L and O_R (either in O_R1-O_R2; or O_R1-O_R2^{inv}; or O_R1^{inv}-O_R2 configuration) separated by 392 basepairs of intervening DNA was used for in vitro transcription. This construct can form a loop between O_R and O_L, which is mostly facilitated by full occupancy of the operator sites (5,26–28). Fig. 6 shows the in vitro transcription results when O_R1-O_R2 sites are in WT and selectively inverted configurations. WT O_R1-O_R2 template shows the expected P_{RM} activation at low CI concentration, and

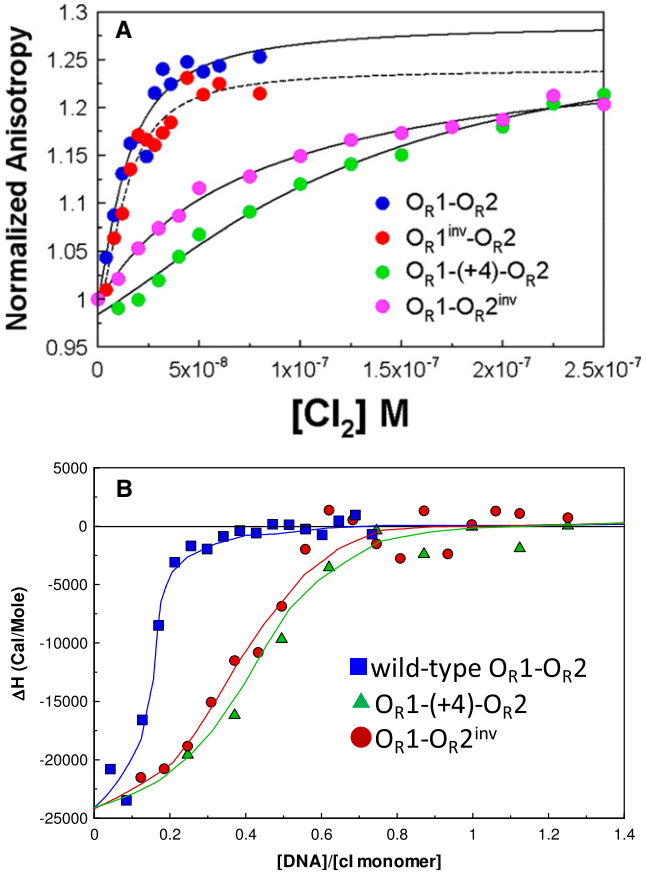

FIGURE 5 (*A*) Binding isotherms of λ-repressor determined from fluorescence anisotropy against indicated oligonucleotides. (*B*) Binding isotherm of λ-repressor and different operator sites containing DNA by isothermal titration microcalorimetry; (■) WT O_R1-O_R2, (▲) O_R1-(+4)-O_R2, and (●) O_R1-O_R2^{inv} containing oligonucleotides.

repression at high CI concentration. Surprisingly, on the O_R1-O_R2^{inv} template, no P_{RM} activation was observed at low CI concentrations. However, at high CI concentrations basal, P_{RM} level was repressed. One possible reason for the loss of P_{RM} activation upon O_R2 inversion is the creation of a mutation (−34G) in the −35 region of P_{RM} from $^{-35}$TAGATA^{-30} to $^{-35}$TGGATA^{-30} (due to the lack of symmetry in the O_R2 sequence). We have restored this mutation from −34G to −34A in the O_R1-O_R2^{inv} sequence and found no P_{RM} activation, but basal level P_{RM} was repressed as before. The basic pattern of P_{RM} activation remains the same in −34G and −34A templates, suggesting that −34G was not solely responsible for the lack of P_{RM} activation. Fig. 6 also shows the effect of O_R1 inversion on P_{RM} activation. The activation was slightly reduced relative to that of the WT O_R1-O_R2 template. The binding and transcription studies indicated that both cooperativity and P_{RM} activation are very sensitive to O_R2 configuration. On the other hand, the change in O_R1 configuration modestly affects CI cooperativity, as well as P_{RM} activation and repression.

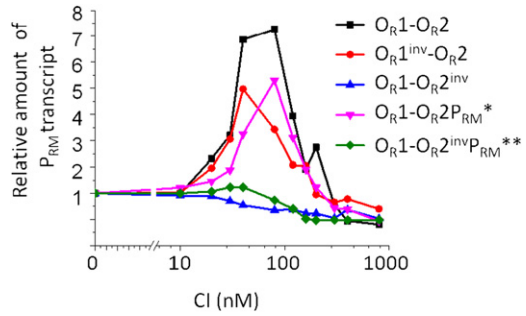

FIGURE 6 Relative in vitro transcription data for different indicated templates. In vitro transcription reactions were carried out as described in the Experimental section. An RNAI transcript (106–108 nucleotides) was used as an internal control to quantify the relative amount of transcripts. The gels were scanned using the ImageQuant program (molecular dynamics) and the ratio of the transcripts area to that of RNAI was calculated to determine the effect of CI on the transcript of interest. The relative transcription refers to values normalized to the zero CI concentration transcripts. P_{RM}* represents a T/A to C/G change at position −34 of P_{RM} in O_R1-O_R2. P_{RM}** represents a C/G to T/A change at position −34 of P_{RM} in O_R1-O_R2^{inv}.

Modeling of operator bound CI

The loss of CI cooperative interaction when bound to O_R1 and O_R2^{inv} raises intriguing questions about the mechanism of this effect. Because inversion of the operator site only changes the relative orientations of the bound proteins, we modeled the change in protein orientation on the DNA. Fig. 7 *A* shows the orientation of the two CI dimers on an oligonucleotide duplex that is identical to the WT O_R1-O_R2 sequence in which the DNA conformation has been assumed to be that of the B-DNA. It can be seen that the two dimers are approximately on the same face of the DNA. Thus, some plausible DNA and protein distortion may be invoked for the establishment of contacts between the C-terminal domains of the two dimers. The DNA distortion has been observed experimentally and the protein-protein contacts have been inferred from the cooperative interaction energy (15,18,29).

Upon O_R2 configuration inversion, the C-terminal domains of CI dimers bound to O_R1 and O_R2^{inv} are almost on the opposite face of the DNA (see Fig. 8 *C*). This makes contacts between the two CI dimers unlikely because of the torsional stiffness of the DNA. It is theoretically possible that the CI dimers may bind in the energetically unfavored orientation on O_R2^{inv} (which would bring the two C-terminal domain onto the same face of DNA again much like the favored orientation in the WT O_R1-O_R2 configuration) and interact with the O_R1 bound repressor cooperatively if energy balance is favorable. To understand this delicate free energy balancing, we define two free energy terms. 1), $\Delta\Delta G^{OR2}{}_{reorient}$, which is the energy needed for the CI to go from favored to unfavored orientation on O_R2; 2), $\Delta G^{12}{}_{loop}$, the net cooperative interaction energy between two O_R1 and O_R2 bound CI dimers. In O_R1-O_R2^{inv},

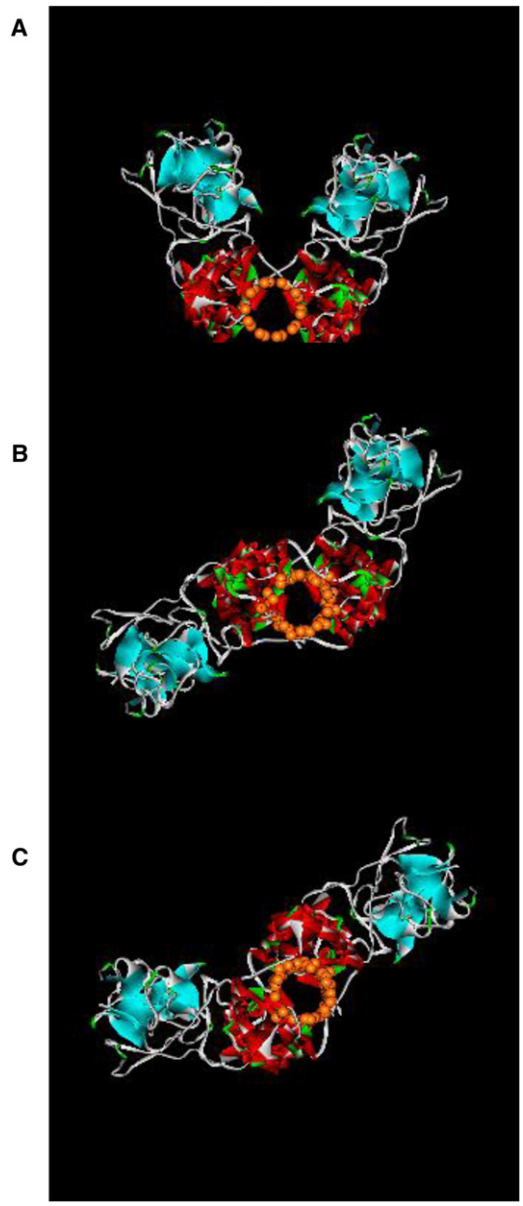

FIGURE 7 Model of two CI dimers bound to (*A*) WT O_R1-O_R2; (*B*) O_R1^{inv}-O_R2; and (*C*) O_R1-O_R2^{inv}. The view is from the axis of the DNA, phosphates of which are represented by orange balls. The helices are in red and the β-sheets are in blue.

the reorientation of the CI dimer on O_R2 and cooperative contact with O_R1 bound CI dimer may occur if the magnitude of the reorientation energy ($|\Delta\Delta G^{OR2}{}_{reorient}|$) is significantly lower than the magnitude of $\Delta G^{12}{}_{loop}$. Clearly, the situation does not occur here suggesting that $|\Delta\Delta G^{OR2}{}_{reorient}| > |\Delta G^{12}{}_{loop}|$. How could O_R1 inversion preserve the cooperative binding (Fig. 7 *B*)? A likely possibility is that the asymmetric CI dimer that preferentially binds the operator site in one orientation (S subunit binds the C-half site), also binds the O_R1 in the other orientation (i.e., S subunit binds the NC half-site), but only moderately weakly (that is $|\Delta\Delta G^{OR1}{}_{reorient}| < |\Delta G^{12}{}_{loop}|$). This would allow the repressor to revert back to native-like spatial orientation on O_R1; compensating the energy loss due to reorientation by interacting with the O_R2 bound CI dimer. The difference in the reorientation energies on O_R1 and O_R2 may stem from the sequence difference between the two sites. We thus hypothesize that this reorientation energy loss is higher for the O_R2-bound CI dimer and cannot be compensated by $\Delta G^{12}{}_{loop}$ (see Discussion and the Supporting Material). Modest effect on cooperative binding is observed upon O_R1 inversion, the magnitude of which is somewhat different in different assays. The source of this variation is not understood.

Origin of the mutual exclusivity of the O_R1-O_R2 and O_R2-O_R3 interaction

We modeled the orientations of the CI dimers on an O_R1-O_R2-O_R3 template (Fig. 8 *A*). As expected, the C-terminal domains of the dimers bound to O_R1 and O_R2 are on the same face of the DNA making cooperative interaction possible. However, the C-terminal domains of the CI dimer bound to O_R3 are on the opposite face of the DNA relative to the C-terminal domains of CI dimer bound at O_R2, making it impossible for O_R2-O_R3 to interact cooperatively. Absence of O_R2-O_R3 cooperativity in the presence of O_R1 is observed in many experimental studies. It is also known that upon deleterious mutations in O_R1, cooperative interactions between O_R2-O_R3 bound dimers occur. How could this happen notwithstanding the unfavorable relative orientations of O_R2 and O_R3 bound dimers (Fig. 8 *B*)? One of

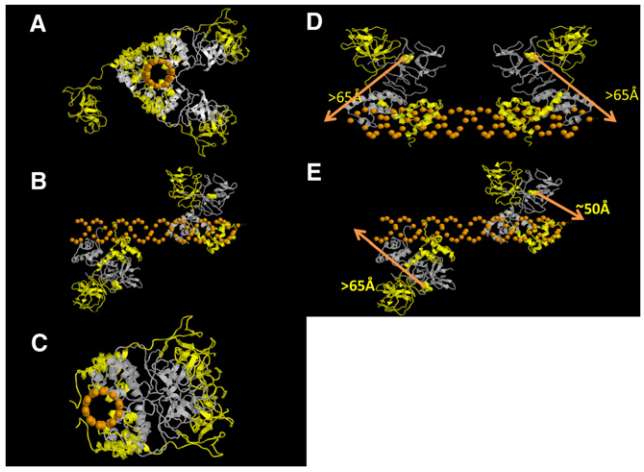

FIGURE 8 (*A*) Represents the O_R1-O_R2-O_R3 bound to three repressor dimers in favored orientations. (*B*) Represents O_R2-O_R3 bound to two repressor dimers in favored orientations. (*C*) Represents O_R2^{inv}-O_R3 bound to two repressor dimers. (*D*) Represents the distances from the Phe-235 of the L subunits to the closest end in O_R2^{inv}-O_R3 configuration. Yellow subunits are the L subunits. (*E*) Represents the distances from the Phe-235 of the L subunits to the closest end in WT O_R2-O_R3 configuration and preferred repressor orientation.

the possibilities is that the CI dimer bound to O_R2 reorient to the unfavorable orientation (S subunit interacting with the NC half-site) and interact with the O_R3-bound dimer. This situation is mimicked in the modeling by inverting the configuration of O_R2 in the O_R2-O_R3 site pair in the model (Fig. 8 *C*). The two C-terminal domain pairs bound to O_R2 and O_R3 now face the same side of the DNA facilitating cooperative interaction. We now define an additional free energy term, $\Delta G^{23}{}_{loop}$, which is the cooperative interaction energy between CI dimers bound to O_R2 and O_R3. Thus, if $|\Delta\Delta G^{OR2}{}_{reorient}|<|\Delta G^{23}{}_{loop}|$, the cooperative interaction between O_R2 and O_R3 can then take place after reorientation of the CI dimer on O_R2 (similar to the O_R1^{inv} situation). This scenario, along with the fact that upon inversion of O_R2, the interaction between CI dimers bound at O_R1 and O_R2 does not occur ($|\Delta\Delta G^{OR2}{}_{reorient}| > |\Delta G^{12}{}_{loop}|$), implies that $|\Delta G^{12}{}_{loop}|<|\Delta\Delta G^{OR2}{}_{reorient}|<|\Delta G^{23}{}_{loop}|$. At this moment, it is not clearly understood why $\Delta G^{23}{}_{loop}$ is larger than $\Delta G^{12}{}_{loop}$. Interestingly, O_R2 and O_R3 are separated by six basepairs, whereas O_R1 and O_R2 are separated by seven basepairs. This results in better alignment and closer approach of the two dimers bound to O_R2 and O_R3 (in the inverted orientation) than the dimers bound to O_R1 and O_R2 (Fig. 7). The closer approach of the two CI dimers should allow contact with each other with less DNA and protein distortion, as well as less sacrifice in energy. This may result in increased magnitude of the $\Delta G^{23}{}_{loop}$ compared to $\Delta G^{12}{}_{loop}$ (see the Supporting Material). It should be noted that $\Delta G^{23}{}_{loop}$ referred to here as the intrinsic cooperative interaction energy for the O_R2- and O_R3-bound dimers, and thus the actual measured energy should be less by the $\Delta\Delta G^{OR2}{}_{reorient}$ energy.

If the orientations of the O_R2-bound repressor are indeed different for O_R1-O_R2 and O_R2-O_R3 cooperativity, it may be reflected in the measured FRET distances. Fig. 8, *D* and *E*, show the distances between the Phe-235 in the L subunit and the modeled position of the end-labeled fluorescence probe. In the orientation where both the O_R2- and O_R3-bound repressor dimers are in the crystal-like orientation (S subunit interacting with the C half-site), the Phe-235 of L subunit in the O_R2 bound repressor dimer is ~50 Å from the modeled position of the end-labeled fluorescence probe. Conversely, in the reoriented position (O_R2-O_R3-bound dimers on the same face of the DNA and S subunit of the O_R2-bound dimer interacting with NC half-site), Phe-235 of both the L subunits are beyond 65 Å from the end-labeled probes (Fig. 8, *D* and *E*).

Figs. 9, *A* and *B*, show FRET from both 5′ and 3′ ends of an O_R2-O_R3 containing oligonucleotide to acrylodan-labeled F235C CI; no significant energy transfer was seen from either DNA ends. This is consistent with the fact that the N-terminal domains of L subunits are facing the central portion of the DNA duplex, away from the ends (Fig. 8 *D*). This result suggests that O_R2-bound repressor in the O_R1-O_R2-bound tetramer must reorient (after dissociating and reassociating) before it is capable of interacting with O_R3-bound repressor dimer. Thus, it appears that the mutual exclusive nature of O_R1-O_R2 cooperativity and O_R2-O_R3 cooperativity originates in the orientation properties of repressor dimers bound to different operator sites. This fine modulation is dependent on the asymmetric nature of the repressor dimer and correct separation of the operator sites.

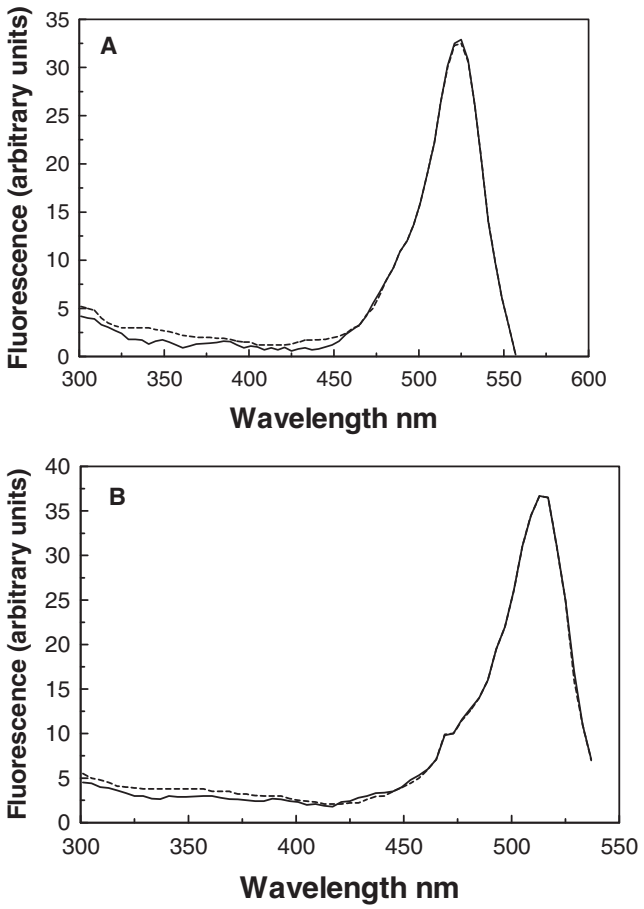

FIGURE 9 FRET shown between acrylodan-labeled Phe-235-Cys repressor complexed with and one-end eosine labeled 42 basepair oligonucleotide duplex containing O_R2-O_R3 sequence in the ratio of 4 (monomer):1(duplex). Figure shows the excitation spectra of eosine-O_R2-O_R3/acrylodan-Phe-235-Cys-repressor complex (*solid line*) and eosin-O_R2-O_R3/Phe-235-Cys repressor complex (*broken line*); (*A*) eosine label nearer to the O_R2 site; (*B*) eosine label nearer to the O_R3 site.

DISCUSSION

Gene regulation, particularly in higher organisms, is carried out by networks of many layers of protein-protein and protein-nucleic acid interactions. Most gene regulatory networks are not simple two-state but multistate switches. How the multistate switches are created from combinations of macromolecular interactions is not well understood. The lysis-lysogeny switch of bacteriophage λ is a simple gene

regulatory network that can be used to understand how multistate switching systems are created. In this study, we focused on a part of this multistate switch that balances stability of the lysogenic state with the ease of induction. This balancing act is accomplished by maintaining the CI concentrations in a narrow range in a single lysogenic cell, which is sufficient to suppress the spontaneous induction without significantly impairing the ease of inducing of the prophage when required.

The CI concentration regulation is accomplished by a CI octamer liganded state in which only one promoter, $P_{RM,}$ is active. The octamer liganded state is required for the establishment of stable lysogeny and is sufficient for the repression of the λ lytic promoters. However, without activation of P_{RM} and synthesis of more CI protein, the induction threshold is low. On the other hand, unregulated expression from P_{RM} causes induction threshold to become too high, causing impairment of induction. Thus, O_R3 probably evolved to generate negative autoregulation to maintain the CI concentration with a narrow range within a lysogenic cell. However, the CI bound O_R3 must not interact with CI bound O_R2 as this would cause instability to the octamer liganded state. We have shown that this mutual exclusivity of CI cooperative binding at O_R1-O_R2 or O_R2-O_R3 is achieved by balancing the protein-protein interaction and reorientation energies (on the operator site), which depends on CI interactions.

How CI orientation dictates the rules of protein-protein interactions may be understood from a more detailed thermodynamic analysis. The relationship of orientation with net protein-protein interaction energy is given by Eq. (1):

$$\Delta G_{loop} = \Delta G_{int} + \Delta G_{prox} + \Delta G_{dis}, \quad (1)$$

where ΔG_{int} is the interaction energy of two isolated protein molecules in solution while remaining bound to isolated binding sites; ΔG_{dis} is the free-energy cost of bringing the undistorted complex to the distorted complex present in the loop; and ΔG_{prox} is the free energy cost due to loss of translational and rotational entropy in a prior step when two isolated molecules interact in solution. The derivations are given in Annexure II of the Supporting Material. From these terms, ΔG_{dis} is strongly orientation dependent making ΔG_{loop} strongly orientation dependent as well. Unless the interaction patches are oriented toward the same face of the DNA, ΔG_{dis} will be prohibitively high, preventing ΔG_{loop} from becoming negative (favorable).

Asymmetry of CI dimer in a dimeric structure causes the C-terminal domains to tilt from the symmetry axis of the N-terminal domains (Fig. S4). In addition, nonequivalence of the two CI monomers along with nonequivalence of the two half-sites within the operator sites creates a free energy difference between the two orientations of the repressor on the operator sites. These structural features, along with the preference for proteins being on the same face of the DNA for cooperative interactions to occur (due to torsional stiffness of DNA) create a situation in which the C-terminal domains of CI bound to O_R1 and O_R2 are on the same face of DNA, whereas the C-terminal domain of CI bound to O_R3 is almost on the other face. This spatial orientation forms the basis of the crucial rule that CI bound to O_R3 cannot interact with the O_R1-O_R2 bound tetramer, thus creating a stable tetrameric and consequently higher order octameric state.

In conclusion, bacteriophage λ has evolved a unique structural solution to create a genetic circuit that balances two mutually exclusive developmental outcomes. As we analyze more complex genetic regulatory circuits, we may encounter structural solutions that are hitherto unknown. Such structural solutions may shed new light on how novel functions arose in respect to gene regulatory networks.

SUPPORTING MATERIAL

Annexure I, Annexure II, Materials and Methods, References, and four figures are available at http://www.biophysj.org/biophysj/supplemental/S0006-3495(12)00169-5.

We acknowledge the Department of Science and Technology, Government of India, for JC Bose Fellowship to S.R., Council of Scientific and Industrial Research for funding the work and fellowship to A.M. This work was also supported by the Intramural Research Program of the National Institutes of Health, the National Cancer Institute, and the Center for Cancer Research.

REFERENCES

1. Elowitz, M. B., and S. Leibler. 2000. A synthetic oscillatory network of transcriptional regulators. *Nature.* 403:335–338.
2. Gardner, T. S., C. R. Cantor, and J. J. Collins. 2000. Construction of a genetic toggle switch in *Escherichia coli*. *Nature.* 403:339–342.
3. Ptashne, M., and A. Gann. 1998. Imposing specificity by localization: mechanism and evolvability. *Curr. Biol.* 8:R812–R822.
4. Ptashne, M. 2005. Regulation of transcription: from lambda to eukaryotes. *Trends Biochem. Sci.* 30:275–279.
5. Dodd, I. B., K. E. Shearwin, …, J. B. Egan. 2004. Cooperativity in long-range gene regulation by the lambda CI repressor. *Genes Dev.* 18:344–354.
6. Ptashne, M. 1992. A Genetic Switch. Cell Press and Blackwell Scientific, Cambridge, MA.
7. Court, D. L., A. B. Oppenheim, and S. L. Adhya. 2007. A new look at bacteriophage lambda genetic networks. *J. Bacteriol.* 189:298–304.
8. Stayrook, S., P. Jaru-Ampornpan, …, M. Lewis. 2008. Crystal structure of the lambda repressor and a model for pairwise cooperative operator binding. *Nature.* 452:1022–1025.
9. Bandyopadhyay, S., S. Deb, …, S. Roy. 2002. Half-of-the-sites reactivity of F235C lambda-repressor: implications for the structure of the whole repressor. *Protein Eng.* 15:393–401.
10. Banik, U., R. Saha, …, S. Roy. 1992. Multiphasic denaturation of the lambda repressor by urea and its implications for the repressor structure. *Eur. J. Biochem.* 206:15–21.
11. Saha, R., U. Banik, …, S. Roy. 1992. An operator-induced conformational change in the C-terminal domain of the lambda repressor. *J. Biol. Chem.* 267:5862–5867.
12. Chatterjee, S., Y. N. Zhou, …, S. Adhya. 1997. Interaction of Gal repressor with inducer and operator: induction of gal transcription from repressor-bound DNA. *Proc. Natl. Acad. Sci. USA.* 94:2957–2962.

13. Cantor, C., and P. Schimmel. 1980. Biophysical Chemistry. W. H. Freeman, San Francisco, CA.

14. Bhattacharya, A., B. Bhattacharyya, and S. Roy. 1996. Fluorescence energy transfer measurement of distances between ligand binding sites of tubulin and its implication for protein-protein interaction. *Protein Sci.* 5:2029–2036.

15. Bandyopadhyay, S., C. Mukhopadhyay, and S. Roy. 1996. Dimer-dimer interfaces of the lambda-repressor are different in liganded and free states. *Biochemistry.* 35:5033–5040.

16. Merabet, E., and G. K. Ackers. 1995. Calorimetric analysis of lambda *cI* repressor binding to DNA operator sites. *Biochemistry.* 34:8554–8563.

17. Lewis, D. E. 2003. Identification of promoters of *Escherichia coli* and phage in transcription section plasmid pSA850. *Methods Enzymol.* 370:618–645.

18. Strahs, D., and M. Brenowitz. 1994. DNA conformational changes associated with the cooperative binding of *cI*-repressor of bacteriophage lambda to OR. *J. Mol. Biol.* 244:494–510.

19. Koblan, K. S., and G. K. Ackers. 1992. Site-specific enthalpic regulation of DNA transcription at bacteriophage lambda OR. *Biochemistry.* 31:57–65.

20. Brenowitz, M., D. F. Senear, …, G. K. Ackers. 1986. "Footprint" titrations yield valid thermodynamic isotherms. *Proc. Natl. Acad. Sci. USA.* 83:8462–8466.

21. Burz, D. S., and G. K. Ackers. 1994. Single-site mutations in the C-terminal domain of bacteriophage lambda cI repressor alter cooperative interactions between dimers adjacently bound to OR. *Biochemistry.* 33:8406–8416.

22. Koblan, K. S., and G. K. Ackers. 1991. Energetics of subunit dimerization in bacteriophage lambda *cI* repressor: linkage to protons, temperature, and KCl. *Biochemistry.* 30:7817–7821.

23. Senear, D. F., and G. K. Ackers. 1990. Proton-linked contributions to site-specific interactions of lambda *cI* repressor and OR. *Biochemistry.* 29:6568–6577.

24. Senear, D. F., M. Brenowitz, …, G. K. Ackers. 1986. Energetics of cooperative protein-DNA interactions: comparison between quantitative deoxyribonuclease footprint titration and filter binding. *Biochemistry.* 25:7344–7354.

25. Meyer, B. J., R. Maurer, and M. Ptashne. 1980. Gene regulation at the right operator (OR) of bacteriophage lambda. II. O_R1, O_R2, and O_R3: their roles in mediating the effects of repressor and cro. *J. Mol. Biol.* 139:163–194.

26. Wang, H., L. Finzi, …, D. Dunlap. 2009. AFM studies of lambda repressor oligomers securing DNA loops. *Curr. Pharm. Biotechnol.* 10:494–501.

27. Lewis, D., P. Le, …, S. Adhya. 2011. Multilevel autoregulation of λ repressor protein CI by DNA looping in vitro. *Proc. Natl. Acad. Sci. USA.* 108:14807–14812.

28. Zurla, C., C. Manzo, …, L. Finzi. 2009. Direct demonstration and quantification of long-range DNA looping by the λ bacteriophage repressor. *Nucleic Acids Res.* 37:2789–2795.

29. Deb, S., S. Bandyopadhyay, and S. Roy. 2000. DNA sequence dependent and independent conformational changes in multipartite operator recognition by lambda-repressor. *Biochemistry.* 39:3377–3383.